Research Article

Journal of Physical Organic Chemistry

Received: 16 April 2008, Revised: 20 May 2008, Accepted: 27 May 2008, Published online in Wiley InterScience: 11 July 2008

(www.interscience.wiley.com) DOI 10.1002/poc.1412

Mechanism of nucleophilic substitutions at phenacyl bromides with pyridines. A computational study of intermediate and transition state

Attila Fábián[a], Ferenc Ruff[a]* and Ödön Farkas[a]*

DFT computations have been performed on nucleophilic substitutions of phenacyl bromides with pyridines to investigate the mechanism of the reaction. In contrast with earlier suppositions, tetrahedral intermediate is not formed by the addition of pyridine on the C═O group of phenacyl bromide, because the total energy of the reacting species increases continuously, when the distance between the N and C(═O) atoms of reactants is shorter than 2.7 Å. At a greater distance, however, a bridged complex of the reactants is observed, in which the N atom of pyridine is slightly closer to the C atom of the C═O, than to the C atom of the CH_2Br group of phenacyl bromide, the distances are 2.87 and 3.05 Å, respectively. The attractive forces between the oppositely polarized N and C(═O) atoms in the complex decrease the free energy of activation of the S_N2 attack of pyridine at the CH_2Br group. The calculated structural parameters of the S_N2 transition states (TS) indicate, that earlier TSs are formed when the pyridine nucleophile bears electron-donating (e-d) groups, while electron-withdrawing (e-w) groups on phenacyl bromide substrate increase the tightness of the TS. Free energies of activation computed for the S_N2 substitution agree well with the data calculated from the results of kinetic experiments and correlate with the σ_{Py} substituent constants, derived for pyridines, and with the Hammett σ constants, when the substituents (4-MeO-4-NO_2) are varied on the pyridine or on the phenacyl bromide reactants. Copyright © 2008 John Wiley & Sons, Ltd.

Supporting information may be found in the online version of this article.

Keywords: nucleophilic substitution; phenacyl bromides; substituent effect; substituent constants for pyridines; free energy of activation; DFT calculations; activation strain analysis

INTRODUCTION

The mechanism of the reactions of phenacyl halides with nucleophiles[1–5] has been investigated by kinetic methods[6–15] for a long time. The reactivity of these substrates proved to be generally higher[16] than that of the alkyl halides. Pearson *et al.*[17] explained the rate enhancement by the electrostatic attraction between the oppositely polarized carbonyl carbon atom of the substrates and the hetero atom of the nucleophiles. At present mainly two proposals for the mechanisms meet with acceptances (Scheme 1). One of them, suggested by Baker[18] and Winstein *et al.*[19] involves the formation of a tetrahedral intermediate (**3**) by the prior addition of the nucleophile on the carbonyl carbon of the phenacyl derivative, and the shift of the nucleophile from C═O to the CH_2 group through a bridged transition state (TS **4**), with the simultaneous expulsion of the leaving group (path A). The other mechanism (path B) involves the S_N2 attack of the nucleophile at the CH_2 group of the substrate and the stabilization of the TS (**6**) through the conjugative effect of the carbonyl group in an enolate form[1,20–26] (**7**). The orbital on the carbon atom, at which displacement takes place, was thought to overlap with the π-orbital of the carbonyl group.[5,26] On the other hand, McLennan and Pross[27] applied the valence-bond configuration mixing model to the nucleophilic substitutions of α-carbonyl derivatives and came to the conclusion that not the enolate form of the C═O group, but the carbanion canonical form of the CH_2 group contributes mainly to the TS of the S_N2 process. S_N2 mechanism was also proposed by Kevill and Kim[28] for the solvolyses of phenacyl derivatives, proceeding with poor nucleophiles in different solvents. Investigating the kinetics of the reaction of substituted phenacyl bromides (**1**) with pyridines (**2**) in acetonitrile and methanol solvents, Lee *et al.*[29–31] found evidences for the first addition-substitution (path A), while Forster and Laird[20,21] for the second S_N2 mechanism (path B).

Not being convinced of the interpretation of the kinetic experiments and of the proposed strange bridged TS (**4**), we have performed DFT computations to test both mechanisms of the reaction of substituted phenacyl bromides (4-MeO-4-NO_2) and pyridines (4′-MeO-4′-NO_2). The results are presented in this paper.

Earlier, we studied the effect of substituents on activation parameters and transition structures of aliphatic nucleophilic

* *Correspondence to: F. Ruff or Ö. Farkas, Department of Organic Chemistry, Institute of Chemistry, L. Eötvös University, P.O. Box 32, H-1518 Budapest 112, Hungary.*
E-mails: ruff@chem.elte.hu; farkas@chem.elte.hu

a *A. Fábián, F. Ruff, Ö. Farkas*
Department of Organic Chemistry, Institute of Chemistry, L. Eötvös University, H-1518 Budapest 112, Hungary

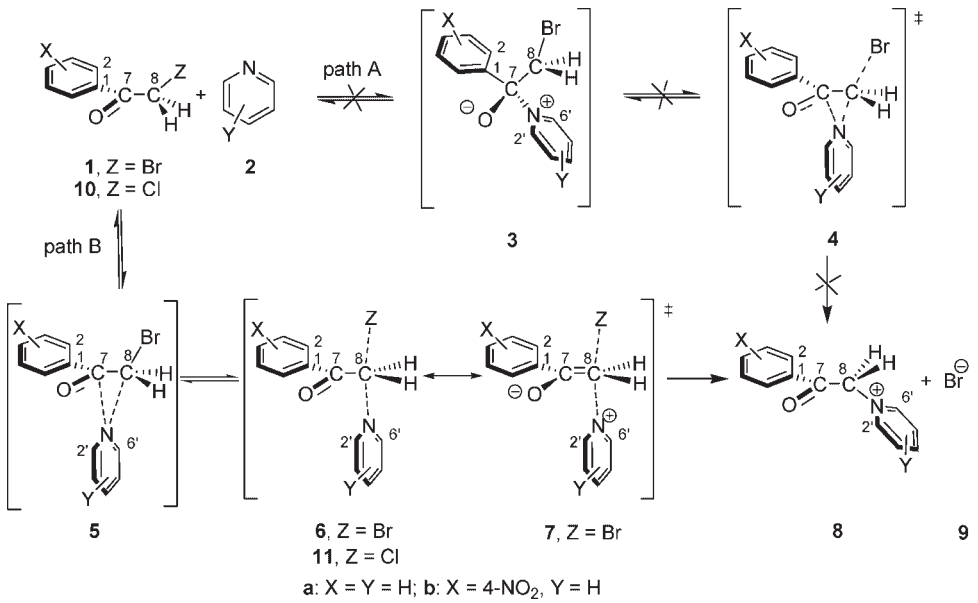

Scheme 1. Mechanism of the reaction of phenacyl bromides (**1**) and phenacyl chlorides (**10**) with pyridines (**2**)

substitutions via DFT computations.[32–34] To validate the results, the computed activation parameters were compared with the data obtained by kinetic experiments. We came to the conclusion that the rearrangement of solvent molecules, which proceeds during the reactions, influences mainly the experimentally derived $\Delta H^{\ddagger}$ and $\Delta S^{\ddagger}$ values, but has minor effect on $\Delta G^{\ddagger}$. Namely the $\Delta H^{\ddagger}$ and $\Delta S^{\ddagger}$ parameters decrease or increase together with solvation, and cancel out each others changes, because equation $\delta\Delta G^{\ddagger} = \delta\Delta H^{\ddagger} - T\delta\Delta S^{\ddagger} \approx 0$ is valid in good approximation. The rearrangement of solvent molecules, however, cannot be computed by applying the polarizable continuum model (PCM) of solvents, therefore, the computed and experimentally derived $\Delta H^{\ddagger}$ and $\Delta S^{\ddagger}$ values may differ considerably from each other. On the other hand, computed and experimental free energies of activations are usually in much better agreement, because the effect of solvent polarity on reactivity can be evaluated well even with the applied simple solvent model, and the effect of solvent rearrangement on experimentally derived $\Delta G^{\ddagger}$ is small.

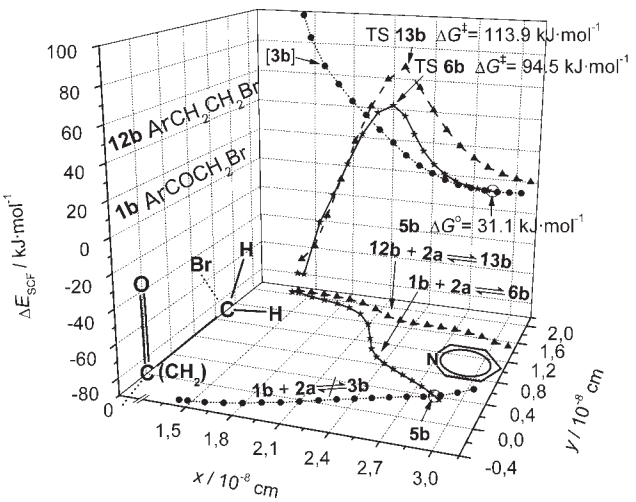

Figure 1. Relaxed potential energy curve trajectories (x-y plane, determined by C(=O), C(H_2Br) and N atoms) and relative total energies (ΔE, z-x plane) for the attack of pyridine (**2a**) on the C=O (**1b** + **2a** ≠ **3b**) and CH_2Br (**1b** + **2a** ⇄ TS **6b**) groups of 4-nitro-phenacyl bromide (**1b**, Scheme 1) and on the CH_2Br (**12b** + **2** ⇄ TS **13b**) group of 2-(4-nitrophenyl)ethyl bromide (**12b**, Scheme 2). Free energy of formation (ΔG°) of complex **5b**, and free energies of activations ($\Delta G^{\ddagger}$) for TSs **6b** and **13b** are 31.1, 94.5 and 113.9 kJ mol^{-1}, respectively. Calculations were performed at DFT(B3LYP)/6-31G(d) level, in methanol, at 310 K

RESULTS AND DISCUSSIONS

Computations have been performed at DFT(B3LYP)/6-31G(d) level in acetonitrile, methanol and water solvents, moreover at DFT(B3LYP)/6-311++G(d,p) level in methanol, applying the PCM of the corresponding solvents (as shown in Computational Methods Section). Selected structural data, total energy and thermodynamic parameters for each species are listed in Tables S1–S7 in the Supplementary Material.

Structure of the intermediate

Potential energy curves have been computed for the attack of pyridine (**2a**) at carbon atoms of both the C=O and the CH_2Br groups of 4-nitrophenacyl bromide (**1b**, Scheme 1), by changing stepwise the $C^7\cdots N$ and $C^8\cdots N$ distances for the reacting molecules. Trajectories of the attacks, and the total energy values at the different scan points, as compared to the reactants, are shown in Fig. 1. The 4-NO_2 group has been attached to phenacyl bromide to promote the formation of tetrahedral intermediate **3b**. The results of computations do not support the formation of intermediate **3** in the attack of the pyridines (**2**) on the carbonyl group of phenacyl bromides (**1**), because the total energy of these species increases steeply with the decrease in the distance between the C^7 and N atoms if they are closer than 2.7 Å (**1b** + **2a** ≠ **3b**, Fig. 1). During the attack of pyridine, the $\theta(NC^7O)$ angle decreases with the decrease of the $R(NC^7)$ distance ($\theta(NC^7O) = -12.7R(NC^7) + 130.3$ ($r = 1.000$); θ and R are given in degree and Å, respectively), and its value corresponds to the

Table 1. Calculated total, strain and interaction energies[39–40] (kJ mol^{-1}) for tetrahedral intermediate **3b** and complex **5b** as well as for TSs **6b** and **13b**, in methanol, at 25 °C

Compound	ΔE	ΔE_{strain}	ΔE_{int}
3b[a]	83.39	148.96	−65.58
5b	−7.84	1.38	−9.22
6b	42.74	94.92	−52.19
13b	65.43	98.25	−32.82

[a] Calculated for scan point $R(C^7N) = 1.500$ Å.

direction of the empty π^* orbital of the C═O group, and to the Bürgi–Dunitz angle.[35–38]

However, the results of DFT computations have showed, that a complex (**5b**) is formed from 4-nitro-phenacyl bromide (**1b**) and pyridine (**2a**) reactants (Scheme 1). Complex **5** has similar structure to the formerly supposed[18,19,29–31] bridged TS **4**, but it is in a minimum and not in a TS on the potential energy surface (Fig. 1). In complex **5b** the N atom is slightly closer to the C═O than to the CH_2 group [$R(C^7N) = 2.87$ Å, $R(C^8N) = 3.05$ Å], and it is situated almost in the same plane as the BrC^8C^7 atoms [$\varphi(BrC^8C^7N) = 168.7°$]. The plane of the pyridine ring is bent towards the oxygen atom of the carbonyl group [$\varphi(OC^8NC^{6'}) = 157.9°$]. The phenacyl moiety of complex **5b** is only slightly distorted ($\varphi(OC^7C^1C^2) = 174.5°$, $\varphi(C^8C^7C^1C^2) = -3.0°$), as compared to the 4-nitrophenacyl bromide (**1b**) reactant ($\varphi(OC^7C^1C^2) = -178.7°$, $\varphi(C^8C^7C^1C^2) = -0.03°$). The free energy of formation of complex **5b** is $\Delta G° = 31.1$ kJ mol^{-1}, the equilibrium constant $K = 5.75 \times 10^{-6}$ (in methanol, at 310 K), therefore the concentration of **5b** is very small in the reaction mixture.

To find the origin of the stabilization or destabilization of the species in path A and B, the 'Activation Strain Analysis', proposed by Bickelhaupt[39,40] was extended to the intermediates. The total energy was decomposed to strain and interaction components ($\Delta E = \Delta E_{strain} + \Delta E_{int}$) and computed for intermediates **3b** and **5b** (Table 1). Complex **5b** can be formed in the reaction, because the strain is very small in this species, and the interaction of the reactants decreases the energy of the system. On the other hand, intermediate **3b** is not formed, because the increase in strain energy is much greater than the decrease in energy, obtained by the interaction of reactants (Table 1).

Structure of the TS

The total energy passes over TS **6b**, and decreases afterwards till the formation of the products, if the *N*-atom of pyridine attacks at the carbon atom of the CH_2Br group of 4-nitrophenacyl bromide (**1b** + **2a** ⇄ TS **6b**, Fig. 1). The trajectory of the relaxed potential energy curve scan is curved towards the carbonyl group and passes through complex **5b**. With the advance of the reaction, the pyridine ring moves away from the C═O and nears towards the CH_2Br group. The attractive interaction between the negatively polarized N atom of pyridine and the positively polarized C^7 atom of the carbonyl group decreases the energy, needed for the nucleophilic substitution at the CH_2Br group, in accordance with the suggestion of Pearson *et al.*[17] Such an effect has not been observed in the trajectory of the reaction of 2-(4-nitrophenyl)ethyl bromide (**12b**) with pyridine

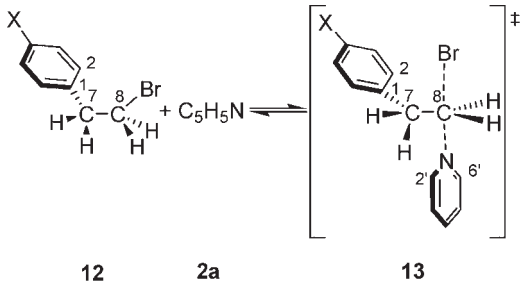

Scheme 2. Mechanism of the reaction of 2-phenylethyl bromides (**12**) with pyridine (**2a**)

(**12b** + **2a** ⇄ TS **13b**, Fig. 1, Scheme 2). TS **13b** of the latter reaction has similar structure but higher energy than TS **6b** of the reaction of 4-nitrophenacyl bromide (**1b**) and pyridine (**2a**). The 'Activation Strain Analysis' [39,40] of the TSs has showed that the strain energies of TSs **6b** and **13b** are similar, but the interaction of the reactants results in a much favourable decrease in energy for TS **6b** than for TS **13b** (Table 1). The similarity of the strain energies suggests that the carbonyl group does not stabilize the distortion of the CH_2Br group of the phenacyl bromide moiety considerably. On the other hand, the differences of the interaction components may indicate the contribution of the empty π^* orbital of the carbonyl group to the stabilization of TS **6b**.

TSs **6** have distorted trigonal bypiramidal (TBP) structure ($\theta(BrC^8N) \approx 175°$, $\theta(C^7C^8N) \approx 92°$, $\theta(C^7C^8Br) \approx 93°$). The plane of the pyridine nucleophile is near to the carbonyl oxygen atom ($\varphi(OC^8NC^{6'}) \approx 145°$). The phenacyl moiety of TS **6** is approximately planar ($\varphi(C^2C^1C^7O) \approx 10.8°$). The C^8Br bond of the leaving bromine and the C^8N bond of the attacking pyridine are almost perpendicular to the plane of the $O{=}C^7{-}C^8$ atoms ($\varphi(OC^7C^8Br) \approx -97.3°$, $\varphi(OC^7C^8N) \approx 83.4°$).

The TS of the nucleophilic substitution reaction of phenacyl bromide (**1a**) and pyridine (**2a**) is slightly early, since bond orders $n = 0.46$ and 0.54 were obtained for the $C^8{\cdots}N$ and $C^8{\cdots}Br$ bonds of TS **6a**, respectively, by using the Pauling equation[41] (Eqn 1). The C—Br and C—N bond lengths (R_o) of phenacyl bromide (**1a**) and *N*-phenacyl pyridinium salt (**8a**), moreover the C···N and C···Br bond distances (R_S) of the symmetric TSs **14** and **15** (Scheme 3) ($n = 0.5$) were used to calculate the *a* constants (Eqn 1). The bond orders were obtained from the $C^8{\cdots}N$ and $C^8{\cdots}Br$ bond distances (R_R) calculated for TS **6a** (Table 2).

$$R - R_0 = a \ln(n) \quad (1)$$

The contribution of enolate **7** (Scheme 1) to TS **6** was investigated by comparing the $R(C^7O)$ and $R(C^7C^8)$ bond lengths, calculated for TS **6a** and for phenacyl bromide (**1a**). The decrease in the $R(C^7C^8)$ and the increase in the $R(C^7O)$ bond lengths are

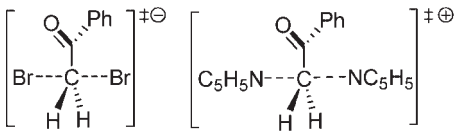

Scheme 3. Symmetric TSs (**14, 15**) of the exchange reactions of phenacyl bromide (**1a**) with bromide ion and N-phenacyl pyridinum ion (**8a**) with pyridine

Table 2. Bond orders (n)[a] calculated for the TS **6a**, generated in the reaction between phenacyl bromide (**1a**) and pyridine (**2a**, Scheme 1)

Solvent	Bond	R_S[b,c]	R_o[c,d]	a[e]	R_R[f]	n
Water	CN	2.037 (**15**)	1.472 (**8a**)	−0.8157	2.106	0.459
	CBr	2.492 (**14**)	1.987 (**1a**)	−0.7281	2.434	0.542
Acetonitrile	CN	2.036 (**15**)	1.472 (**8a**)	−0.8136	2.100	0.462
	CBr	2.491 (**14**)	1.987 (**1a**)	−0.7279	2.439	0.537
Methanol	CN	2.037 (**15**)	1.472 (**8a**)	−0.8152	2.099	0.464
	CBr	2.491 (**14**)	1.987 (**1a**)	−0.7281	2.439	0.538

[a] Bond orders were calculated according to Pauling (Eqn 1).
[b] Atomic distances (Å) calculated for symmetric TSs ($n = 0.5$).
[c] The numbers of the relating species are given in parentheses.
[d] Bond lengths (Å) calculated for reactant or product.
[e] Constant calculated for Eqn 1.
[f] Atomic distances (Å) calculated for TS **6a**.

expected in the TS at a significant contribution of the enolate, and $\Delta R(C^7C^8) = -0.021$ Å and $\Delta R(C^7O) = 0.0030$ Å were found for the difference of the corresponding bond distances of **6a** and **1a**. In the reaction of 2-phenylethyl bromide (**12a**) with pyridine (**2a**), $\Delta R(C^7C^8) = -0.0125$ Å was obtained from the data calculated for TS **13a** and reactant **12a**. In this latter reaction the shortening of the C^7—C^8 bond can be explained with the change of the hybridization state of the C^8 atom from sp^3 towards sp^2 at the formation of TS **13a**. Though the increase in the C^7═O bond length during the formation TS **6a** is very small, the somewhat greater shortening of the $R(C^7C^8)$ bond lengths for TS **6a** than for TS **13a** may refer to a resonance interaction with the C═O group in TS **6a**. A greater contribution of the enolate form **7** would be expected for TSs bearing electron-donating (e-d) groups on the pyridine ring.[22,23] Accordingly, the greatest negative charge for the carbonyl oxygen (Q(O)), and the shortest $R(C^7C^8)$ bond distance were obtained for these derivatives (Fig. 2). To sum it up, the results may refer to a small but significant contribution of enolate **7** to TS **6**.

Structural parameters, calculated for TSs **6** of the reactions of phenacyl bromide ($C_6H_5COCH_2Br$, **1a**) with substituted pyridines (YC_5H_4N, **2**) have been plotted against σ_{Py} substituent constants, derived for pyridines (as shown in Section Computational Methods). The Q(Br) negative charge of the leaving bromine, the $R(C^8Br)$ and $R(C^7C^8)$ distances and the $\theta(C^7C^8N)$ angle increase, while the Q(O) negative charge of the carbonyl oxygen, the $R(C^8N)$ distance and the $\theta(C^7C^8Br)$ angle decrease, with the increase in the electron-withdrawing (e-w) effect and σ_{Py} constant of the Y substituents of pyridine (Fig. 2 and Figures S1–S5 in the Supplementary Material for data obtained in different solvents). All these structural changes are consequences of the formation of more product like TSs with the increasing e-w effect of the substituent of pyridine.

Structural parameters, calculated for the reaction of substituted phenacyl bromides ($XC_6H_4COCH_2Br$, **1**) with pyridine (C_5H_5N, **2a**), give linear correlations with the Hammett σ constants. The values of all structural parameters ((Q(Br), Q(O), $R(C^8Br)$, $R(C^8N)$, $\theta(C^7C^8N)$, $\theta(C^7C^8Br)$, $R(C^7O)$ and $R(C^7C^8)$) decrease with the increasing e-w effect of the X substituents of the phenacyl moiety (Fig. 3 and Figures S6–S8 in the Supplementary Material for data obtained in different solvents). The structures of the TSs **6** become tighter and have less distorted TBP geometry with the increasing e-w effect of the X substituents of phenacyl bromides.

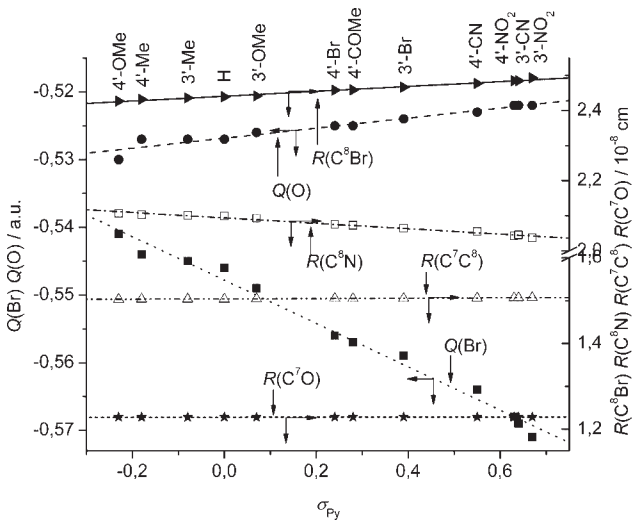

Figure 2. Plots of charges (Q(Br), Q(O)) and bond distances ($R(C^8Br)$, $R(C^8N)$, $R(C^7C^8)$, $R(C^7O)$) of TSs **6** against the σ_{Py} constants for the reaction of phenacyl bromide ($PhCOCH_2Br$, **1a**) with substituted pyridines (YC_5H_4N, **2**), calculated at DFT(B3LYP)/6-31G(d) level, in acetonitrile, at 318 K. (Correlations: $Q(Br) = -0.0325\sigma_{Py} - 0.548$ ($r = 0.995$); $Q(O) = 0.00755\sigma_{Py} - 0.527$ ($r = 0.976$); $R(C^8Br) = 0.0704\sigma_{Py} + 2.441$ ($r = 0.995$); $R(C^8N) = -0.00783\sigma_{Py} + 2.095$ ($r = 0.991$); $R(C^7O) = 0.000175\sigma_{Py} + 1.228$ ($r = 0.373$); $R(C^7C^8) = 0.00429\sigma_{Py} + 1.504$ ($r = 0.990$). Correlations for plots given in Figure S1: $\theta(C^7C^8Br) = -2.63\sigma_{Py} + 92.6$ ($r = 0.990$); $\theta(C^7C^8N) = 3.07\sigma_{Py} + 92.0$ ($r = 0.992$))

Effect of substituents on reactivity

Activation parameters were computed at DFT(B3LYP)/6-31G(d) level in acetonitrile, methanol and water, moreover at DFT(B3LYP)/6–311++ G(d,p) level in methanol, and compared with the data calculated from the results of kinetic experiments performed in acetonitrile,[29] methanol[20,21] and 90% acetone–

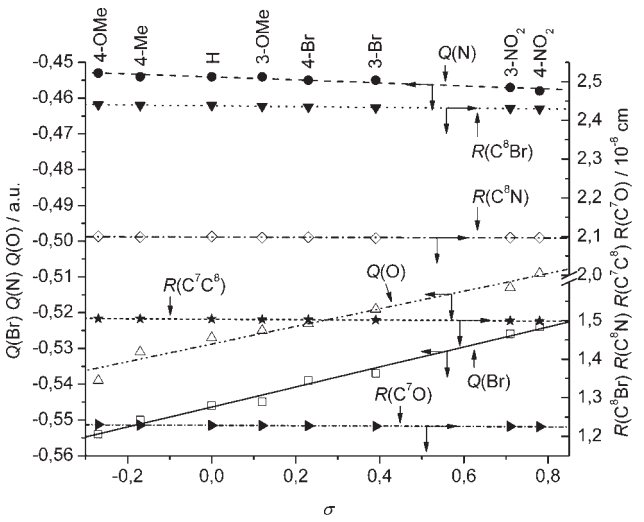

Figure 3. Plots of charges (Q(Br), Q(O), Q(N)) and bond distances (R(C^{8}Br), R(C^{8}N), R(C^{7}C^8), R(C^{7}O)) of TSs **6** against the Hammett σ constants for the reaction of substituted phenacyl bromides ($XC_6H_4COCH_2Br$, **1**) with pyridine (C_5H_5N, **2a**), calculated at (B3LYP)/6-31G(d) level, in acetonitrile, at 318 K. (Correlations: $Q(Br) = 0.0280\sigma - 0.546$ ($r = 0.994$); $Q(O) = 0.0247\sigma - 0.529$ ($r = 0.982$); $Q(N) = -0.00421\sigma - 0.454$ ($r = 0.957$); $R(C^8Br) = -0.0103\sigma + 2.438$ ($r = 0.986$); $R(C^8N) = -0.00344\sigma + 2.099$ ($r = 0.774$); $R(C^7C^8) = -0.00590\sigma + 1.503$ ($r = 0.996$); $R(C^7O) = -0.00474\sigma + 1.229$ ($r = 0.968$); correlations for plots given in Figure S5: $\theta(C^7C^8Br) = -1.69\sigma + 92.7$ ($r = 0.974$); $\theta(C^7C^8N) = -0.101\sigma + 92.0$ ($r = 0.261$))

water mixtures,[42] respectively. The activation parameters were correlated with the Hammett σ constants, and with the σ_{Py} substituent constants, derived for pyridines.

In the reactions of phenacyl bromide (**1a**) with substituted pyridines (**2**, Scheme 1) the e-d effect of the Y substituents increase the nucleophilicity of pyridine, and the rate of the reactions, that is decrease the free energy of activation (Figs 4 and 5 and Figure S9, Table 3, Nos. 1, 4 and 7 for data obtained in different solvents). The experimentally derived[29] $\Delta G^{\ddagger}$ values give a broken plot against the Hammett σ constants in acetonitrile (**6**(σ,exp) plot in Fig. 4). Such a change of reactivity with the substituent constants has been explained[43–49] by the change of the rate determining-step in multi-step reactions. The reactivities of the pyridine nucleophile and the leaving bromide ion are very similar, in the Swain–Scott equation[50–52] their nucleophilic constants are $n = 3.6$ and 3.5, respectively. Pyridine and its derivatives, bearing e-d groups are better nucleophiles, while those derivatives bearing e-w substituents are poorer nucleophiles than bromide ion. Therefore, it has been suggested by Lee *et al.*,[29] that in the reaction of phenacyl bromide with good pyridine nucleophiles, the rate-determining step is the formation of tetrahedral intermediate **3**, while with poor pyridine nucleophiles the rate-determining step changes for the breakdown of intermediate **3**. However, the $\Delta G^{\ddagger}$ *versus* σ plot, computed for the S_N2 mechanism of this reaction (**1a** + **2** ⇄ TS **6**) is also broken, though no break would be expected for a single-step S_N2 reaction; (**6**(σ,calc) and **6**(σ,exp) plots in Fig. 4). The results of computations demonstrate that assuming a tetrahedral intermediate is not necessary. Moreover the calculated $\Delta G^{\ddagger}$ *versus* σ plot for the S_N2 reaction of phenacyl chloride with substituted pyridines (**10a** + **2** ⇄ TS **11**) is also broken at the very same σ value as that of the phenacyl bromide (**11**(σ,calc) and **6**(σ,calc) plots in Fig. 4), though the nucleophilicity

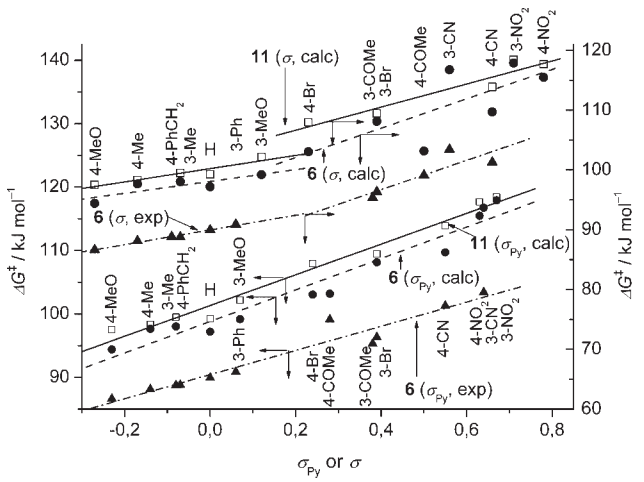

Figure 4. Calculated and experimentally derived[29] $\Delta G^{\ddagger}$ *versus* σ, and $\Delta G^{\ddagger}$ *versus* σ_{Py} plots for the reactions of phenacyl bromide (**1a** + **2** ⇄ TS **6**) and phenacyl chloride (**10a** + **2** ⇄ TS **11**) with pyridines (**2**) in acetonitrile, at 318 K. Calculations were performed at DFT(B3LYP)/6-31G(d) level. (Correlations for $\Delta G^{\ddagger}$ *versus* σ_{Py} plots are given in Table 3, Nos. 1 and 10)

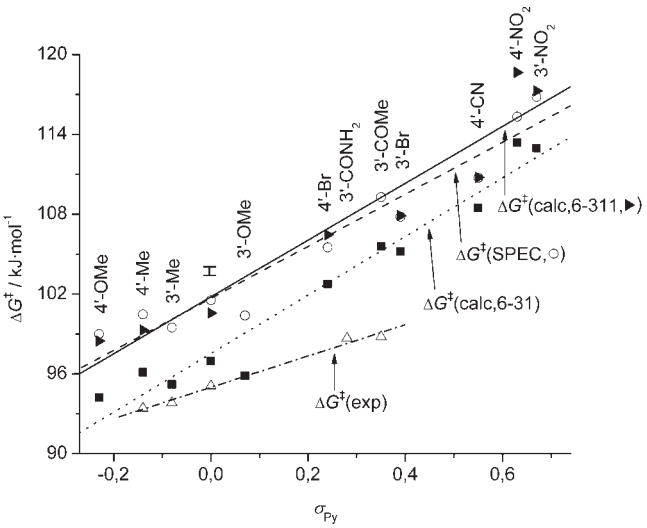

Figure 5. Calculated and experimentally derived[20,21] $\Delta G^{\ddagger}$ *versus* σ_{Py} plots for the reaction of phenacyl bromide with pyridines (**1a** + **2** ⇄ TS **6**) in methanol, at 310 K. Calculations were performed at DFT(B3LYP)/6-31G(d) and DFT(B3LYP)/6-311++G(d,p) levels with optimization or with single point energy calculations (SPEC). (Correlations are given in Table 3, No. 4)

of the chloride ion ($n = 2.7$) is much smaller than that of the bromide ion. If the change of the relative nucleophilicities of the nucleophile and the leaving group were the reason for the break of the $\Delta G^{\ddagger}$ *versus* σ plots, than the breaks of the plots for the reactions of phenacyl bromide (TS **6**) and phenacyl chloride (TS **11**) would be at different σ values.

The resonance interaction between the orthogonally positioned π orbital of the 4-substituents and the lone pair of the N atom of pyridine is very different from the interaction, which occurs at the dissociation of benzoic acids, used for the determination of the σ constants. This difference is the cause of the break of the $\Delta G^{\ddagger}$ *versus* σ plots. Therefore, instead of

Table 3. Correlations for the calculated and experimentally derived[20,21,29,42] $\Delta G^{\ddagger}$, $\Delta H^{\ddagger}$ and $\Delta S^{\ddagger}$ activation parameters against the σ_{Py} and σ substituents constants for the reactions of phenacyl bromide (**1a** + **2** ⇄ TS **6**) and phenacyl chloride (**10a** + **2** ⇄ TS **11**) with pyridines (**2**), moreover for substituted phenacyl bromides with pyridine (**1** + **2a** ⇄ TS **6**, Scheme 1)

				$\Delta P^{\ddagger} = \delta\Delta P^{\ddagger}\sigma + \Delta P^{\ddagger}_{o}$ $(r; N)$[b]	
No.	Reaction	Solvent	T/K[a]	Calculated[c]	Experimental
1	**1a** + **2** ⇄ TS **6**	Acetonitrile	318	$\Delta G^{\ddagger} = 24.8\sigma_{Py} + 98.8$ (0.972; 12)	$\Delta G^{\ddagger} = 19.0\sigma_{Py} + 90.4$ (0.969; 11)
2				$\Delta H^{\ddagger} = 24.3\sigma_{Py} + 49.4$ (0.988; 12)	—
3				$\Delta S^{\ddagger} = -1.80\sigma_{Py} - 157$ (0.105; 12)	—
4	**1a** + **2** ⇄ TS **6**	Methanol	310	$\Delta G^{\ddagger} = 22.1\sigma_{Py} + 97.5$ (0.977; 11)[d]	$\Delta G^{\ddagger} = 11.8\sigma_{Py} + 95.0$ (0.994; 5)
5				$\Delta H^{\ddagger} = 23.3\sigma_{Py} + 49.7$ (0.989; 11)	$\Delta H^{\ddagger} = 7.53\sigma_{Py} + 60.7$ (0.675; 5)
6				$\Delta S^{\ddagger} = 4.32\sigma_{Py} - 156$ (0.370; 11)	$\Delta S^{\ddagger} = -13.6\sigma_{Py} - 110$ (0.488; 5)
7	**1a** + **2** ⇄ TS **6**	Water	308	$\Delta G^{\ddagger} = 19.5\sigma_{Py} + 95.8$ (0.986; 11)	$\Delta G^{\ddagger} = 16.6\sigma_{Py} + 91.6$ (0.992; 6)[e]
8				$\Delta H^{\ddagger} = 22.4\sigma_{Py} + 48.2$ (0.991; 11)	—
9				$\Delta S^{\ddagger} = 9.53\sigma_{Py} - 155$ (0.691; 11)	—
10	**10a** + **2** ⇄ TS **11**	Acetonitrile	318	$\Delta G^{\ddagger} = 24.2\sigma_{Py} + 101$ (0.989; 10)	—
11				$\Delta H^{\ddagger} = 23.1\sigma_{Py} + 50.7$ (0.990; 10)	—
12				$\Delta S^{\ddagger} = -2.81\sigma_{Py} - 159$ (0.525; 10)	—
13	**1** + **2a** ⇄ TS **6**	Acetonitrile	318	$\Delta G^{\ddagger} = -2.47\sigma + 97.2$ (0.718; 8)	$\Delta G^{\ddagger} = -1.64\sigma + 89.7$ (0.983; 6)
14				$\Delta H^{\ddagger} = -2.75\sigma + 48.1$ (0.975; 8)	—
15				$\Delta S^{\ddagger} = -0.90\sigma - 154$ (0.113; 8)	—
16	**1** + **2a** ⇄ TS **6**	Methanol	310	$\Delta G^{\ddagger} = -3.68\sigma + 96.7$ (0.874; 8)	$\Delta G^{\ddagger} = -1.53\sigma + 95.1$ (0.997; 6)
17				$\Delta H^{\ddagger} = -3.02\sigma + 48.4$ (0.987; 8)	$\Delta H^{\ddagger} = 4.14\sigma + 61.1$ (0.709; 6)
18				$\Delta S^{\ddagger} = 2.11\sigma - 156$ (0.293; 8)	$\Delta S^{\ddagger} = 18.3\sigma - 110$ (0.814; 6)

[a] Temperature of calculations and experiments.
[b] $P = G$, H or S; σ = The Hammett σ constants or the σ_{Py} constants; determined for pyridines; r = correlation coefficient; N = number of compounds.
[c] Calculated at DFT(B3LYP)/6-31G(d) level if not otherwise stated.
[d] At DFT(B3LYP)/6-311++G(d,p) level with optimization, $\Delta G^{\ddagger} = 21.4\sigma_{Py} + 102$ (0.964; 8); At DFT(B3LYP)/6-311++G(d,p) level with SPEC approximation; $\Delta G^{\ddagger} = 19.5\sigma_{Py} + 102$ (0.969; 9).
[e] Experimental data were measured in 90% acetone–water.[42]

the Hammett σ constants, the σ_{Py} parameters, calculated from the dissociation constants of pyridinium ions,[53,54] must be used for the reactions of 4-substituted pyridines (as shown in Section Computational Methods). The Hammett σ_m constants are valid for the reactions of 3-substituted pyridines because the resonance effect between the 3-substituent and the N atom is poor.[55] The σ_{Py} substituent constants, calculated for resonance e-d and e-w 4-substituents of pyridine, are larger and smaller, respectively, than the Hammett σ_p constants, because both e-d and e-w resonance effects of 4-substituents are less effective in the pyridine ring than in the case of the benzene derivatives. Resonance e-w 4-subtstituents (e.g. 4-COMe, 4-CO_2Me, 4-CN, 4-NO_2) proved to be weakly e-d, when stabilizing a positively polarized centre.[56–58] Better correlations are obtained for the calculated $\Delta G^{\ddagger}$ data of TSs **6** and **11** and for the experimental $\Delta G^{\ddagger}$ values of TS **6** if they are plotted against the σ_{Py} constants (**6**(σ_{Py},calc), **6**(σ_{Py},exp) and **11**(σ_{Py},calc) plots in Fig. 4, as shown in moreover plots in Fig. 5 and Figure S9 and data in Table 3, Nos. 1, 4 and 7, obtained in different solvents). The σ_{Py} constants, however, may also slightly depend on reactions of pyridines, especially in the case of 4-MeO, 4-Me and 3-MeO groups.[59–62] In the TSs of the S_N2 reactions, the π electrons of the pyridine ring may interact with the C—C bonds of the substrate, for example with the C^7—C^8 bond of phenacyl derivatives. Such an interaction does not take place in protonation of pyridines, used for the determination of the σ_{Py} constants.

The substituent effect is smaller in the reaction of phenacyl bromide (**1a**) with substituted pyridines (**2**) than in the dissociation of pyridinium ions, reaction constants $\delta\Delta G^{\ddagger} \sim 20\,kJ\,mol^{-1}\sigma_{Py}^{-1}$ ($\rho \sim -3.3$) and $\delta\Delta G^{\circ} = -36.4\,kJ\,mol^{-1}\sigma_{Py}^{-1}$ ($\rho = 6.01$) were calculated for the slope of the ΔG *versus* σ_{Py} plots, respectively ($\delta\Delta G = -2.303RT\rho$;[32] Table 3, Nos. 1, 4, 7 and 10). Computed $\delta\Delta G^{\ddagger}$ data are in the best agreement with the results measured in the aprotic acetonitrile (Table 3, No 1, **6**(σ_{Py},calc), **6**(σ_{Py},exp) plots in Fig. 4). In protic solvents the experimentally derived $\delta\Delta G^{\ddagger}$ data are smaller than the calculated ones (e.g. in methanol $\delta\Delta G^{\ddagger} = 11.8$ and $22.1\,kJ\,mol^{-1}\sigma_{Py}^{-1}$, respectively, Table 3, No 4 and 7, Fig. 5 and Figure S9). The substituent effect in alkylations of pyridines was also found to be smaller in protic solvents.[59] Good pyridine nucleophiles form stronger hydrogen bonding, which decreases their reactivity to a greater extent than in the case of poor nucleophiles. The effect of hydrogen bonds was not taken into consideration, by using the PCM of solvents, therefore computed $\delta\Delta G^{\ddagger}$ data do not depend on solvent significantly (Table 3, Nos. 1, 4 and 7). The deviation of the measured and calculated $\Delta G^{\ddagger}$ values is less than $8\,kJ\,mol^{-1}$

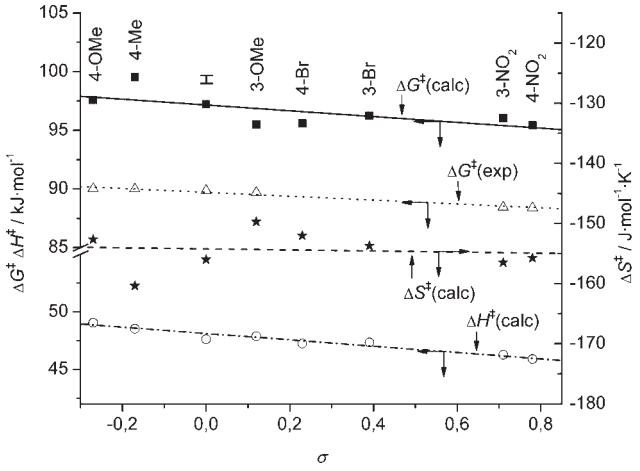

Figure 6. Calculated $\Delta G^{\ddagger}/\Delta H^{\ddagger}/\Delta S^{\ddagger}$ *versus* σ, and experimentally derived[29] $\Delta G^{\ddagger}$ *versus* σ plots for the reaction of substituted phenacyl bromides ($XC_6H_4COCH_2Br$, **1**) with pyridine (C_5H_5N, **2a**) in acetonitrile, at 318 K. Calculations were performed at DFT(B3LYP)/6-31G(d) level. (Correlations are given in Table 3, Nos. 13-15)

(Figs 4, 5 and Figure S9). Experimental data are in best agreement with the results obtained at the lower DFT(B3LYP)/6-31G(d) level, but $\Delta G^{\ddagger}$ data computed at different levels with optimization or with single point energy calculations (SPEC) do not deviate from each other considerably (Fig. 5).

In the reactions of substituted phenacyl bromides (**1**) with pyridine (**2a**) the e-w X groups of the substrate accelerate the reactions and decrease the $\Delta G^{\ddagger}$ values, which give linear correlations with the Hammett σ constants (Figs 6 and 7). The substituents of the benzene ring are far from the centre of the reaction and this is the reason why reactivity is changed with the substituents only to a small extent (as shown in slopes of $\Delta G^{\ddagger}$ *versus* σ plots in Table 3, Nos. 13 and 16). Earlier the minor effect of substituents was explained[29] with the supposed small changes

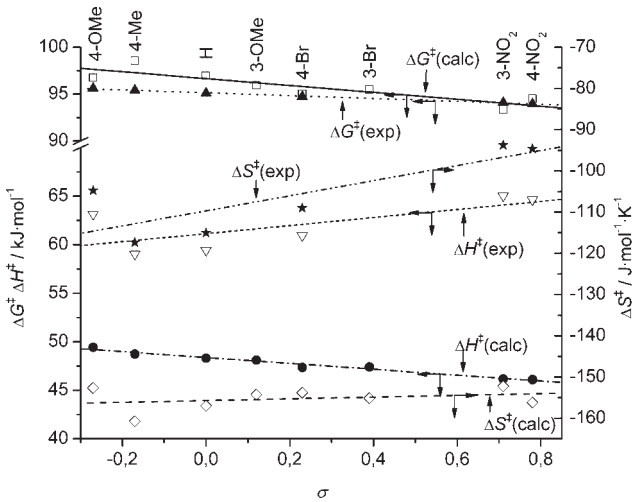

Figure 7. Calculated and experimentally derived[29] $\Delta G^{\ddagger}/\Delta H^{\ddagger}/\Delta S^{\ddagger}$ *versus* σ plots for the reaction of substituted phenacyl bromides ($XC_6H_4COCH_2Br$, **1**) with pyridine (C_5H_5N, **2a**) in methanol, at 310 K. Calculations were performed at DFT(B3LYP)/6-31G(d) level. (Correlations are given in Table 3, Nos. 16–18)

of charges in the reaction. The same magnitude of changes were calculated for charges of bromine and oxygen atoms for the reactions of substituted phenacyl bromides with pyridine ($\delta\Delta Q(Br) = 0.0280$ a.u. σ^{-1}, $\delta\Delta Q(O) = 0.0247$ a.u. σ^{-1} Fig. 3) and phenacyl bromide with substituted pyridines ($\delta\Delta Q(Br) = 0.0325$ a.u. σ_{Py}^{-1}, $\delta\Delta Q(O) = 0.00755$ a.u. σ_{Py}^{-1} Fig. 2], though the changes of reactivity are very different in these two series of reactions (as shown in slopes of $\Delta G^{\ddagger}$ *versus* σ plots in Table 3, Nos. 1, 4, 7, 13 and 16). It seems that the change of reactivity and the change of charges are not correlated. The small absolute value of the $\delta\Delta G^{\ddagger}$ reaction constants for the reactions of substituted phenacyl bromides with pyridine ($\delta\Delta G^{\ddagger} \sim -1.6$ kJ mol$^{-1}\sigma^{-1}$; $\rho \sim 0.26$; Table 3, Nos. 13 and 16) also support the attack of pyridine on the CH_2Br group of phenacyl bromide.[63] Similar reaction constant were observed in the nucleophilic substitution reactions of 2-arylethyl and phenacyl derivatives, proceeding by S_N2 mechanism.[11,12,20,21,29–31,63–66] Much greater reaction constants ($\rho \sim 2$) were obtained if the nucleophilic addition takes place on a carbonyl group coupled to a benzene ring.[67–71]

The charges, formed in the TS, influence the solvation and the experimentally derived $\Delta S^{\ddagger}$ values. In the reaction of substituted phenacyl bromides (**1**) with pyridine (**2a**), the measured $\Delta S^{\ddagger}$ values increase with the increasing e-w effect of the X substituents ($\delta\Delta S^{\ddagger} = 18.3$ J mol^{-1} K$^{-1}\sigma^{-1}$, Table 3, No. 18, Fig. 7) because the negative charge of bromine and therefore the solvation decrease at the formation of the TS in the given series of compounds (Fig. 3). On the other hand, in the reactions of phenacyl bromide (**1a**) with substituted pyridines (**2**), the negative charge of bromine (Fig. 2) and the solvation increases, the experimentally derived $\Delta S^{\ddagger}$ data decrease ($\delta\Delta S^{\ddagger} = -13.6$ J mol^{-1} K$^{-1}\sigma_{Py}^{-1}$, Table 3, No. 6, Figure S10) with the increase of the e-w effect of the Y substituents. The values of experimentally derived $\Delta H^{\ddagger}$ parameters are also influenced by the change of $\Delta S^{\ddagger}$, that is by the solvation.[32–34] The rearrangements of the solvent molecules, which occur during the reactions, are not included in our calculations, therefore the computed $\Delta S^{\ddagger}$ data depend only slightly on the substituents of the pyridine or phenacyl bromide reactants (Table 3, Nos. 3, 6, 9, 12, 15 and 18, Fig. 7 and Figure S10), and the slope of the computed $\Delta G^{\ddagger}$ *versus* σ and $\Delta H^{\ddagger}$ *versus* σ plots are very similar. (For the calculated data, $\delta\Delta G^{\ddagger} \approx \delta\Delta H^{\ddagger}$.) Though, the deviation of the calculated and experimentally derived $\Delta H^{\ddagger}$ and $\Delta S^{\ddagger}$ values can be considerable, the corresponding $\Delta G^{\ddagger}$ data agree with each other, owing to the compensation effect of the solvent rearrangement.[32–34]

CONCLUSIONS

DFT calculations do not support the addition of pyridine on the carbonyl group of phenacyl bromides, that is the formation of the tetrahedral intermediate **3** (Scheme 1), because the total energy and the free energy of the reacting species increase continuously with the decrease in the distance between the N and C^7 atoms, if they are closer than 2.7 Å (Fig. 1). However, the attraction between the positively polarized C^7 atom of the carbonyl group of phenacyl bromides and the negatively polarized N atom of the pyridine nucleophiles promote the formation of complex **5** at distances greater than 2.7 Å. The formation of complex **5** opens a pathway of smaller energy for the S_N2-type TS **6**, and decreases the free energy of activation for the nucleophilic substitution on the CH_2Br group. This may be the reason why nucleophilic

substitutions on phenacyl substrates proceed faster than the analogous reactions of alkyl halides of similar structure. The enolate form **7** seems also to make a significant contribution to the stability of TS **6**. All the reactions pass through the S_N2 type TS **6**, the structure of which changes with the substituents. The reaction coordinate of the TS increases with the increase in the e-w effect of the substituents of pyridine, while these groups on phenacyl bromide reactants increase the tightness of the TS. Owing to the restricted resonance effects, the subtituent effect in the reaction of 4-substituted pyridine derivatives can be evaluated properly only by using the σ_{Py} substituent constants, derived from dissociation constants of pyridinium ions.

When discussions of experimental data of mechanistic studies lead to controversial conclusions, quantum chemical computations may efficiently contribute to more reliable decisions.

COMPUTATIONAL METHODS

The geometry of the compounds was fully optimized without symmetry constraints by use of the Gaussian 03 software package[72] at DFT(B3LYP)/6-31G(d) level in acetonitrile, methanol and water solvents, at 318, 310 and 305 K, respectively. Temperatures are the same as used in the corresponding kinetic measurements. Optimizations and SPEC were also carried out at DFT(B3LYP)/6-311++G(d,p) level in methanol. The chosen B3LYP functional was found to perform well in investigation of trends in nucleophilic substitution reactions.[73,74] The solvent effect was incorporated by applying the PCM[75] in the integral equation formalism[76,77] (IEF-PCM) of the corresponding solvent. Relaxed potential energy curve scans were made by changing the N···C=O and N···CH_2Br distances stepwise, to calculate the pathways for the attacks of the pyridine nucleophile (**2a**) on C=O and CH_2Br groups of 4-nitrophenacyl bromide (**1b**) and on the CH_2Br group of 2(4-nitrophenyl)ethyl bromide (**12b**). Structures were characterized as energy minima or TSs by calculating the harmonic vibrational frequencies, with the use of analytical second derivatives. No or one imaginary frequency was obtained for reactants and TSs, respectively. Selected data for the optimized structures obtained by means of DFT calculations are listed in Tables S1–S3, in the Supplementary Material.

The sums of the electronic and thermal free energies (*G*) and enthalpies (*H*) and also the entropies of formation (*S*) for reactants and TSs were obtained by the standard procedure in the framework of the harmonic approximation,[78,79] and are listed together with the calculated total energies (*E*) and numbers of imaginary frequencies in Tables S4–S7 in the Supplementary Material. The computed entropy values, obtained in solutions, agree with the data calculated by application of Benson's rule[80,81] in the gas phase. As an example, the *S* value of 411.3 J mol^{-1} K^{-1} was obtained for $C_6H_5COCH_2Br$ (**1a**) by DFT calculations in solution. In comparison, a values of S = 425 J mol^{-1} K^{-1} was calculated on application of Benson's rule.

The $\Delta E^{\ddagger}$ $\Delta G^{\ddagger}$, $\Delta H^{\ddagger}$, $\Delta S^{\ddagger}$ activation parameters of the reactions were calculated from the differences in the *E*, *G*, *H* and *S* values of the TSs or scan points and reactants, respectively (Eqn 2, $P = E$, *G*, *H* or *S*).

$$\Delta P^{\ddagger} = P_{TS} - \sum P_R \qquad (2)$$

The generated $\Delta E^{\ddagger}$, $\Delta G^{\ddagger}$ and $\Delta H^{\ddagger}$ values were multiplied by 2625.5 in order to convert them from atomic into kJ mol^{-1} units.

Experimentally derived activation parameters for the reactions were calculated from the second order rate constants ($k_2 = k_1$/[Nuc]). The activation parameters, obtained through DFT computations and from kinetic measurements, were correlated with the substituent constants (Eqn 3, $P = G$, *H*, or *S*), as described previously.[32–34]

$$\Delta P^{\ddagger} = \delta\Delta P^{\ddagger}\sigma + \Delta P_o^{\ddagger} \qquad (3)$$

The $\delta\Delta P^{\ddagger}$ reaction constants characterize the effect of substituents on activation parameters, $\Delta P^{\ddagger}$ and $\Delta P_0^{\ddagger}$ are the activation parameters of substituted and unsubstituted compounds, respectively. The Hammett σ constants[82] were used in the correlations of the reactions of substituted phenacyl bromides with pyridine. For the reactions of phenacyl bromide with substituted pyridines, the σ_{Py} substituent constants were calculated by Eqn (4) using the method of Fischer *et al*.[53,54] (In Reference [53,54], σ_{Py} is referred to as 'effective substituent constant', and denoted by $\overline{\sigma}$.)

$$\sigma_{Py} = (pK_a^o - pK_a)/\rho \qquad (4)$$

The pK_a^0 and pK_a data of pyridine and its substituted derivatives, respectively, were determined[53] in water, at 25 °C. $\rho = 6.01$ was calculated from the slope of the linear plot of the pK_a values of 3-substituted pyridine derivatives against the Hammett σ_m constants. The σ_{Py} substituent constants for 4-substituted derivatives were calculated with this ρ reaction constant and their pK_a values. The σ_{Py} constants may also depend on the reaction, and in some cases slightly larger values for 4-MeO and 4-Me groups (−0.12 and −0.09 instead of −0.23 and −0.14, respectively) and a smaller one for 3-MeO group (0.04 instead of 0.07) were found to be more appropriate.[54,62] The σ and σ_{Py} constants, used in the correlations are listed in Table S8 in the Supplementary Material.

SUPPORTING INFORMATION

Plots of calculated structural data against the substituent constants, selected atomic charges, bond distances and angles as well as calculated total energies, sums electronic and thermal free energies and enthalpies, entropies of formation and number of imaginary frequencies are listed in the supporting information, which can be found in the online version of this article.

Acknowledgements

The authors thank Professor Árpád Kucsman for fruitful discussions. This work was supported by the Hungarian Scientific Research Foundation and GVOP (OTKA No. K 60889 and GVOP-3.1.1-2004-05-0451/3.0).

REFERENCES

[1] M. J. S. Dewar, *The Electronic Theory of Organic Chemistry*. Oxford University Press, Oxford, **1949**, p. 73.
[2] E. L. Eliel, *Steric Effect in Organic Chemistry*, (Ed.: M. S. Newman). Wiley, New York, **1956**, p. 103.
[3] J. Hine, *Physical Organic Chemistry* (2nd edn), McGraw-Hill, New York, **1962**. p. 176.
[4] C. A. Bunton, *Nucleophilic Substitution at a Saturated Carbon Atom*, Elsevier, London, **1963**, p. 35.

[5] E. M. Kosower, *An Introduction to Physical Organic Chemistry*, Wiley, New York, **1968**. pp. 77–79.
[6] F. G. Bordwell, W. T. Brannen, *J. Am. Chem. Soc.* **1964**, *86*, 4645–4650.
[7] S. D. Ross, M. Finkelstein, R. C. Petersen, *J. Am. Chem. Soc.* **1968**, *90*, 6411–6415.
[8] J. W. Thorpe, J. Warkentin, *Can. J. Chem.* **1973**, *51*, 927–935.
[9] L. M. Litvinenko, L. A. Perelman, *Zh. Org. Khim.* **1967**, *3*, 936–941.
[10] L. M. Litvinenko, L. A. Perelman, *Reakt. Sposob. Org. Soedin.* **1971**, *8*, 331–342.
[11] I. Lee, C. S. Shim, S. Y. Chung, H. W. Lee, *J. Chem. Soc. Perkin Trans. 2* **1988**, 975–981.
[12] I. Lee, C. S. Shim, H. W. Lee, *J. Phys. Org. Chem.* **1989**, *2*, 484–490.
[13] S. J. Winston, P. J. Rao, B. Sethuram, T. N. Rao, *Indian J. Chem. Section A* **1996**, *35A*, 979–982.
[14] M. K. Pillay, R. Jeyaraman, M. Nallu, P. Venuvanalingam, M. Ramalingam, *Indian J. Chem. Section A* **1997**, *36A*, 414–417.
[15] J.-L. M. Abboud, R. Notario, J. Bertran, M. Sola, *Prog. Phys. Org. Chem.* **1993**, *19*, 104–181.
[16] A. Halvorsen, J. Songstad, *J. Chem. Soc. Chem. Commun.* **1978**, 327–328.
[17] R. G. Pearson, S. H. Langer, F. V. Williams, W. J. McGuire, *J. Am. Chem. Soc.* **1952**, *74*, 5130–5132.
[18] J. W. Baker, *Trans. Faraday Soc.* **1941**, *37*, 632–641.
[19] S. Winstein, E. Grunwald, H. W. Jones, *J. Am. Chem. Soc.* **1951**, *73*, 2700–2707.
[20] W. Forster, R. M. Laird, *J. Chem. Soc. Perkin Trans. 2* **1982**, 135–138.
[21] W. Forster, R. M. Laird, *J. Chem. Soc. Perkin Trans. 2* **1991**, 1033–1044.
[22] T. L. Yousaf, E. S. Lewis, *J. Am. Chem. Soc.* **1987**, *109*, 6137–6142.
[23] D. Kost, K. Aviram, *Tetrahedron Lett.* **1982**, 4157–4160.
[24] I. Lee, I. C. Kim, *Bull. Korean Chem. Soc.* **1988**, *9*, 133–135.
[25] I. Lee, S. W. Hong, J. H. Park, *Bull. Korean Chem. Soc.* **1989**, *10*, 459–462.
[26] D. M. Kalendra, B. R. Sickles, *J. Org. Chem.* **2003**, *68*, 1594–1596.
[27] D. J. McLennan, A. Pross, *J. Chem. Soc. Perkin Trans. 2* **1984**, 981–984.
[28] D. N. Kevill, C-B. Kim, *J. Org. Chem.* **2004**, *70*, 1490–1493.
[29] H. J. Koh, K. L. Han, H. W. Lee, I. Lee, *J. Org. Chem.* **2000**, *65*, 4706–4711.
[30] I. Lee, H. W. Lee, Y. K. Yu, *Bull. Korean Chem. Soc.* **2003**, *24*, 993–997.
[31] K. S. Lee, K. K. Adhikary, H. W. Lee, B-S. Lee, I. Lee, *Org. Biomol. Chem.* **2003**, *1*, 1989–1994.
[32] F. Ruff, Ö. Farkas, *J. Org. Chem.* **2006**, *71*, 3409–3416.
[33] F. Ruff, Ö. Farkas, Á. Kucsman, *Eur. J. Org. Chem.* **2006**, 5570–5580.
[34] F. Ruff, Ö. Farkas, *J. Phys. Org. Chem.* **2008**, *21*, 53–61.
[35] H. B. Bürgi, J. R. Dunitz, E. J. Shefter, *J. Am. Chem. Soc.* **1973**, *95*, 5065–5067.
[36] H. B. Bürgi, J. M. Lehn, G. Wipff, *J. Am. Chem. Soc.* **1974**, *96*, 1956–1957.
[37] H. B. Bürgi, J. R. Dunitz, J. M. Lehn, G. Wipff, *Tetrahedron* **1974**, *31*, 1563–1570.
[38] E. L. Eliel, S. H. Wilen, *Stereochemistry of Organic Compounds*, Wiley, New York, **1994**, p. 685, 737, 877.
[39] F. M. Bickelhaupt, *J. Comput. Chem.* **1999**, *20*, 114–128.
[40] G. T. de Jong, F. M. Bickelhaupt, *ChemPhysChem.* **2007**, *8*, 1170–1181.
[41] L. Pauling, *J. Am. Chem. Soc.* **1947**, *69*, 542–553.
[42] A. Shunmugasundaram, S. Balakumar, *Indian J. Chem. Section A* **1985**, *24A*, 775–777.
[43] Broken, concave downwards log *k* vs. σ Hammett plots are widely regarded[44–49] to be diagnostic for the change of the rate-determining step with the substituents in multi-step reactions. The analogous $\Delta G^{\ddagger}$ vs. σ plots are concave upwards (like the upper three plots in Fig. 4), as their slopes are the opposite of the slopes of the log *k* vs. σ plots, because the greater the rate of a reaction the smaller the free energy of activation. However it must be mentioned, that curved log *k* vs. pK_a plots have also been interpreted by Jencks *et al.*[49] to result from changes of the structure of the TS in single-step reaction.
[44] O. Exner, *Advances in Linear Free Energy Relationships*, (Eds: N. B., Chapman, J. Shorter,) Plenum Press, London, **1972**, Ch 1.
[45] R. A. Y. Jones, *Physical and Mechanistic Organic Chemistry*, Cambridge University Press, Cambridge, **1984**, pp. 43–45.
[46] N. S. Isaacs, *Physical Organic Chemistry*, Longman-Harlow, England, **1987**, pp. 146–148.
[47] F. Ruff, I. G. Csizmadia, *Organic Reactions, Equilibria, Kinetics and Mechanism*, Elsevier, Amsterdam, **1994**, pp. 170-177.
[48] J. Clayden, N. Greeves, S. Warren, P. Wothers, *Organic Chemistry*, Oxford University Press, Oxford, **2001**, pp. 1090–1100.
[49] W. P. Jencks, S. R. Brant, J. R. Gandler, G. Fendrich, C. Nakamura, *J. Am. Chem. Soc.* **1982**, *104*, 7045–7051.
[50] C. G. Swain, C. B. Scott, *J. Am. Chem. Soc.* **1953**, *75*, 141–147.
[51] P. R. Wells, *Chem. Rev.* **1963**, *63*, 171–219.
[52] J. Koskikallio, *Acta Chem. Scand.* **1969**, *23*, 1477–1490.
[53] A. Fischer, W. J. Galloway, J. Vaughan, *J. Chem. Soc.* **1964**, 3591–3596.
[54] A. Fischer, W. J. Galloway, J. Vaughan, *J. Chem. Soc.* **1964**, 3596–3599.
[55] J. A. Zoltewicz, *Adv. Heterocycl. Chem.* **1978**, *22*, 71–121.
[56] E. V. Anslyn, D. A. Dougherty, *Modern Physical Organic Chemistry*, University Science Books, Sausalito, **2006**. p. 655.
[57] I. Lee, C. K. Kim, I. S. Han, H. W. Lee, W. K. Kim, Y. B. Kim, *J. Chem. Phys. B* **1999**, *103*, 7302–7307.
[58] S. W. Hong, H. J. Koh, I. Lee, *J. Phys. Org. Chem.* **1999**, *12*, 425–429.
[59] C. D. Johnson, I. Roberts, P. G. Taylor, *J. Chem. Soc. Perkin Trans. 2* **1981**, 409–413.
[60] R. Gallo, C. Roussel, *Adv. Heterocycl. Chem.* **1988**, *43*, 191–193.
[61] K. J. Schaper, *Arch. Pharm.* **1978**, *311*, 641–650.
[62] K. Clarke, K. Rothwell, *J. Chem. Soc.* **1960**, 1885–1893.
[63] C. Srinivasan, A. Shunmugasundarum, N. Arumugam, *J. Chem. Soc. Perkin Trans. 2* **1985**, 17–19.
[64] S.-D. Yoh, K.-H. Yang, I.-S. Han, *Tetrahedron* **1987**, *43*, 4089–4096.
[65] S.-D. Yoh, O.-S. Lee, *Tetrahedron Lett.* **1988**, *29*, 4431–4434.
[66] O.-S. Lee, S.-D. Yoh, *Bull. Korean Chem. Soc.* **1985**, *6*, 99–102.
[67] H. H. Jaffe, *Chem. Rev.* **1953**, *53*, 191–261.
[68] W. P. Jencks, *Prog. Phys. Org. Chem.* **1964**, *2*, 63–118.
[69] W. J. Bover, P. Zuman, *J. Chem. Soc. Perkin Trans. 2* **1973**, 786–790.
[70] M. P. Crampton, *J. Chem. Soc. Perkin Trans. 2* **1975**, 185–189.
[71] R. A. Y. Jones, *Physical and Mechanistic Organic Chemistry*, Cambridge University Press, Cambridge, **1984**, p. 269.
[72] M. J. Frisch, G. W. Trucks, H. B. Schlegel, G. E. Scuseria, M. A. Robb, J. R. Cheeseman, J. A. Montgomery, Jr., T. Vreven, K. N. Kudin, J. C. Burant, J. M. Millam, S. S. Iyengar, J. Tomasi, V. Barone, B. Mennucci, M. Cossi, G. Scalmani, N. Rega, G. A. Peterson, H. Nakatsuji, M. Hada, M. Ehara, K. Toyota, R. Fukuda, J. Hasegawa, M. Ishida, T. Nakajima, Y. Honda, O. Kitao, H. Nakai, M. Klene, X. Li, J. E. Knox, H. P. Hartchian, J. B. Cross, C. Adamo, C. Jaramillo, R. Gomperts, R. E. Stratmann, O. Yazyev, A. J. Austin, R. Cammi, C. Pomelli, J. W. Ochterski, P. Y. Ayala, K. Morokuma, G. A. Voth, P. Salvador, J. J. Dannenberg, V. G. Zakrzewski, S. Daprich, A. D. Daniels, M. C. Strain, Ö. Farkas, D. K. Malick, A. D. Rabuck, K. Raghavachari, J. B. Foresman, J. V. Ortiz, Q. Cui, A. G. Baboul, S. Clifford, J. Cioslowski, B. B. Stefanov, G. Liu, A. Liashenko, P. Piskorz, I. Komáromi, R. L. Martin, D. J. Fox, T. Keith, L. A. Al-Laham, C. Y. Peng, A. Nanayakkara, M. Challacombe, P. M. W. Gill, B. Johnson, W. Chen, M. W. Wong, C. Gonzalez, J. A. Pople, *Gaussian 03, Revision B.01, Gaussian Inc., Pittsburg, PA, 2003.*
[73] A. P. Bento, M. Sola, F. M. Bickelhaupt, *J. Comput. Chem.* **2005**, *26*, 1497–1504.
[74] M. Swart, M. Sola, F. M. Bickelhaupt, *J. Comput. Chem.* **2007**, *28*, 1551–1560.
[75] J. Tomasi, M. Persico, *Chem. Rev.* **1994**, *94*, 2027–2094.
[76] E. Cancès, B. Mennucci, *J. Chem. Phys.* **2000**, *114*, 4744–4745.
[77] D. M. Chipman, *J. Chem. Phys.* **2000**, *112*, 5558–5568.
[78] D. A. McQuarrie, J. D. Simon, *Molecular Thermodynamics*, University Science Books, Sausalito, CA, **1999**.
[79] http://www.gaussian.com/g_whitepap/thermo/thermo.pdf
[80] S. W. Benson, F. R. Cruickshank, D. M. Golden, G. R. Haugen, H. E. O'Neal, A. S. Rodgers, R. Shaw, R. Walsh, *Chem. Rev.* **1969**, *69*, 279–290.
[81] S. W. Benson, *Thermochemical Kinetics*, Wiley, New York, **1976**. pp. 19–72.
[82] C. Hansch, H. Leo, R. W. Taft, *Chem. Rev.* **1991**, *91*, 165–195.